ORIGINAL ARTICLE

Silencing of nuclear factor kappa b 1 gene expression inhibits colony formation, cell migration and invasion via the downregulation of interleukin 1 beta and matrix metallopeptidase 9 in renal cell carcinoma

Luiz Felipe S. Teixeira[1] · Jean Pierre S. Peron[2] · Maria Helena Bellini[1]

Abstract

Renal cell carcinoma (RCC) is a highly deadly urological tumor due to its high metastatic incidence and its notorious chemoresistance. The nuclear transcription factor kappa B (NF-κB) family has been associated with apoptosis resistance and cellular invasion in RCC. The purpose of this study was to evaluate the impact of NF-κB1 gene silencing on the colony formation, cell migration and invasion abilities of the RCC cell line. Renca–mock and Renca-shRNA-NF-κB1 cells were used in this work. NF-κB1 downregulation was assessed by western blotting. The mRNA expression levels of interleukin-1 beta (IL-1β) and MMP-9 were assessed by real-time quantitative polymerase chain reaction (RT-qPCR). The IL-1β levels in the culture media were determined by a commercial ELISA kit. The MMP-9 protein expression and gelatinolytic activity were evaluated by western blotting and zymography, respectively, and the migration and invasion abilities were analysed. The expression levels of p105 and p50 in Renca-shRNA-NF-κBmoc1 cells were significantly reduced compared with those in the Renca–mock cells. The colony numbers of shRNA-NF-κB1 cells were lower than the colony numbers of the Renca–mock cells. NF-κB1 knockdown inhibited the cell migration and invasion of Renca-shRNA-NF-κB1 cells. These cells also exhibited reduced levels of IL-1β. The MMP-9 expression and activity levels were significantly reduced in Renca-shRNA-NF-κB1 cells. Taken together, these results indicate that the downregulation of NF-κB1 suppresses the tumourigenicity of RCC by reducing MMP-9 expression and activity; thus, NF-κB1 could be a molecular target for RCC treatment.

Keywords Renal cell carcinoma · NF-κB1 · shRNA · IL-1β · MMP-9 · Colony formation · Migration · Invasion

Introduction

Renal cell carcinoma (RCC) accounts for 90–95% of the kidney cancer cases, and approximately 25–30% of patients with RCC develop metastasis after surgery [1, 2]. These patients have a relatively low 5-year survival rate of less than 10% [3]. The histological subcategory of RCC occuring with the highest frequency is Clear cell RCC (ccRCC) [4]. Almost 85% of sporadic ccRCC has the Von Hippel–Lindau (VHL) tumour suppressor gene mutated, deleted or epigenetically silenced. The loss of VHL function leads to a constitutively active hypoxia-inducible factor alpha (HIFα) pathway. Additionally, the inactivation of VHL was shown to activate nuclear factor kappa B (NF-κB), a family of transcription factors that promotes tumour growth [5, 6]. Researchers have confirmed that this transcription factor is expressed in almost all cell types and regulates many genes with roles related to pathological processes, such as inflammation, oxidative stress, apoptosis, cell survival, invasion, and migration [7].

Mammals are known to exhibit these five menbers of the Rel/NF-κB family: RelA (p65), RelB, c-Rel, NF-κB1 (p105/p50) and NF-κB2 (p100/p52). NF-κB1-p105 and NF-κB2-p100 are precursor molecules that, when cleaved from the N-terminal region of the proteasome (26S), generate mature proteins: p50 and p52 [7]. NF-κB-regulated

✉ Maria Helena Bellini
  mhmarumo@terra.com.br

1 Department of Biotechnology, IPEN-CNEN/SP, 2242
  Av. Lineu Prestes, Cidade Universitária, Butantã,
  São Paulo 05508-000, Brazil

2 Immunology Department, ICB IV, University of São Paulo,
  São Paulo, Brazil

products, such IL-6, TNF, IL-1, and chemokines are major mediators of inflammation [8]. In the tumour milieu, IL-1 induces the expression of various metastatic mediators, such as matrix metalloproteinases (MMP), VEGF, IL-8, IL-6, TNF-α, and TGFβ [9].

The involvement of p50 in carcinogenesis has been demonstrated in vitro [10] and in clinical studies [11]. There is a positive correlation between the histological grade, invasion, and metastasis with NF-κB1 activation in RCC [12, 13]. In addition, it has been reported that p50 promoter polymorphisms (− 94 ins/del ATTG, rs28362491) are associated with an increased risk of RCC [14].

Metastasis is a multi-step process involving the proteolytic degradation of the basement membrane, cellular migration, and invasion through the barrier into secondary sites [15]. The degradation of the matrix in the basement membrane is largely controlled by extracellular proteinases, such as the matrix metalloproteinases (MMPs) [16]. MMPs are overexpressed in almost all cancers, including RCC [17]. Among them, the increased expression of MMP-9, which is transcriptionally regulated by NF-κB, has been correlated with a poor prognosis for RCC [18]. Thus, the aim of this study was to evaluate the impact of the downregulation of the NF-κB1 gene on the colony formation, cellular migration and invasion abilities of the murine renal cell adenocarcinoma cell line.

Materials and methods

Cell lines

The RCC cell line used (Renca) was obtained from American Type Culture Collection (catalogue no: CRL-2947™, Manassas, VA, USA). Renca–mock and Renca-shRNA-NF-κB1 cells were both obtained by our laboratory. In brief, Short hairpin ribonucleic acid (ShRNA) targeting NF-κB1 messenger ribonucleic acid (mRNA) and the empty vector were packet into HEK 293T cells. The concentrate lentivirus supernatant of these cells was then used to transduce Renca cells. After that, puromycin was added to the culture media to select resistant clones [19].

All cell lines were cultured in RPMI-1640 (Gibco® Invitrogen, Grand Island, NY, USA) medium supplemented with 10% foetal bovine serum (FBS) (Gibco®, Invitrogen, Grand Island, NY, USA), 100 U/ml penicillin and 100 µg/ml streptomycin (Gibco® Invitrogen, Grand Island, NY, USA) in a humidified incubator with 5% CO_2 at 37 °C. [19].

RNA extraction and RT-qPCR

Total cellular RNA was extracted with TRIzol® (Life Technologies, Carlsbad, CA, USA). Next, the cDNA was synthesized with the QuantiTect® Reverse Transcription Kit (Qiagen, Hilden, Germany) according to the manufacturer's protocol using 2 µg of RNA, and the cDNA was stored at − 20 °C. Absolute SYBR Green qPCR Mix® (Invitrogen, Carlsbad, CA, USA) was used according to the manufacturer's instructions. The reactions were carried out in a 10 µl volume reaction system. The PCR conditions consisted of 40 cycles, with a 15 s denaturation at 95 °C, a 1 h annealing at 60 °C and a 1 min elongation step at 72 °C. The target gene expression levels were normalized to the GAPDH mRNA levels. The primers used were as follows: MMP-9, forward: 5′-CAAGTGGGACCATCATAACATCA-3′ and reverse: 5′-CTCGCGGCAAGTCTTCAGA-3′; IL-1β, forward: 5′-AGTTGACGGACCCCAAAAGAT-3′ and reverse: 5′-GGACAGCCCAGGTCAAAGG-3′; GAPDH, forward: 5′-GCCTTCCGTGTTCCTACCC-3′ and reverse: 5′-TGA AGTCGCAGGAGACAACC-3′. The relative quantification of gene expression was performed with the $2^{−ΔΔCT}$ method (13). PCR was carried out using the ABI-Prism 7000 quantitative PCR instrument (Applied Biosystems Company, Foster City, CA, USA).

Protein extraction and western blotting analysis

The protein contents were extracted from the cells and were prepared with the CelLytic™ M reagent (Sigma-Aldrich, St Louis, MO, USA). After centrifugation, the supernatant was collected and added to Protease Inhibitor Cocktail powder (Sigma-Aldrich, St Louis, MO, USA). The protein concentration was detected by the bicinchoninic acid assay (BCA) method and was stored at − 80 °C until required for use. The protein was loaded at a concentration of 50 µg per lane, separated by 12% SDS-PAGE and transferred onto GE Hybond-P polyvinyl difluoride (PVDF) membranes, which were then blocked in 5% skim milk in Tris–buffered saline at room temperature for 1 h. The membranes were incubated overnight at 4 °C with the following primary antibodies: anti-NF-κB1 p105/p50 (rabbit monoclonal anti-mouse; Abcam, Cambridge, UK), anti-MMP-9 goat polyclonal (Santa Cruz Biotechnology, Dallas, Texas, USA), Anti-IL-1β goat polyclonal (Sigma-Aldrich, St Louis, MO, USA) and anti-GAPDH (MAB374 mouse monoclonal; Millipore, Massachusetts, USA), all diluted 1:500; then the membranes were incubated with the following HRP-conjugated secondary antibodies: goat anti-rabbit (Santa Cruz Biotechnology, Texas, USA), donkey anti-goat (Santa Cruz Biotechnology, Texas, USA) and goat anti-mouse (Invitrogen, CA, USA), all diluted 1:1000, for 2 h at room temperature. The anti-GAPDH antibody was used as a loading control. To detect the Western blot signals, the SuperSignal® West Pico Chemiluminescent Substrate Kit (Thermo Scientific, Waltham, USA) was used. Photos were taken using the

Uvitec Cambridge Alliance 4.7 equipment. The results were quantified using ImageJ software.

Colony formation assay

Renca cells were seeded (1×10^2 cells) onto 60 mm plates containing RPMI medium with 10% FBS and were maintained in growth conditions for 10 days. Then, the plates were washed twice with PBS, fixed and stained with 3 ml of 2% formaldehyde/4% rhodamine B (Synth, SP, Brazil) for 20 min. After this, the plates were washed with distilled water, and the colonies were manually counted.

Wound healing assay

Renca cells were seeded into six-well plates (4×10^5 cells/well). Once the cells reached 90% confluence, a wound area was carefully created by scraping the cell monolayer with a sterile 1000 µl pipette tip. The cells were then washed once with PBS to remove the detached cells. Subsequently, the cells were incubated at 37 °C in 5% carbon dioxide. The width of the wound area was monitored with an inverted microscope at various time points. The cells that migrated to the lower compartment of the membrane were photographed on the inverted Nikon Eclypse 100 microscope for cell quantification using ImageJ software; then, the following formula was used to calculate the percentage of migrated area: % = (Area 0 h − Area 48 h)/(Area 0 h) × (100).

Transwell migration assay

Transwell chambers (BD Biosciences, Bedford, MA, USA) with 2 mm diameter polycarbonate filters and 8 µm pores were used. Renca cells (2×10^5 cells/chamber) were resuspended in 100 µL of RPMI medium without FBS and were transferred to the Transwell chambers that were placed in 24-well plates containing RPMI medium with FBS, which functioned as a chemotactic solution. After incubation for 48 h, the chambers were washed with PBS, fixed with 3.7% formaldehyde for 2 min, washed with PBS, and permeabilized with 100% methanol for 20 min. The methanol was removed by washing with PBS, and the cells were stained with 1% Giemsa stain (Synth, SP, BRA) for 15 min. The cells retained in the upper membrane compartment were removed with a cotton swab. The cells that migrated to the lower compartment of the membrane were photographed on an inverted Nikon Eclipse E100 microscope for cell quantification using ImageJ software.

Transwell invasion assay

Transwell chambers (BD Biosciences, Bedford, MA, USA) with 2 mm diameter polycarbonate filters and 8 µm pores were used. Matrigel (Corning, Bedford, MA, USA) was diluted in RPMI free of fetal bovine serum (FBS) in a 1:10 proportion (32 µg/ml) and was then incubated for 1 h for gel polymerization. Renca cells (2×10^5 cells/chamber) were resuspended in 100 µL of RPMI medium without FBS and were transferred to the Transwell chambers that were placed in 24-well plates containing RPMI medium with FBS, which functioned as a chemotactic solution. After incubation for 48 h, the chambers were washed with PBS, fixed with 3.7% formaldehyde for 2 min, washed with PBS, and permeabilized with 100% methanol for 20 min. The methanol was removed by washing with PBS, and the cells were stained with 1% Giemsa stain (Synth, SP, BRA) for 15 min. The cells retained in the upper membrane compartment were removed with a cotton swab. The cells that migrated to the lower compartment of the membrane were photographed on an inverted Nikon Eclypse 100 microscope for cell quantification using ImageJ software.

Zymography

Gelatine zymography was performed as follows: polyacrylamide gels (SDS-PAGE, 10%) were copolymerized with gelatine (0.1%) (Sigma-Aldrich). For each sample, 25 µl of serum-free conditioned media and sample buffer (without β-mercaptoethanol) were loaded into the gel well. Electrophoresis was performed in the presence of SDS at a constant voltage of 100 V. Following electrophoresis, the gels were washed twice in 2.5% Triton X-100 for 15 min in an orbital shaker. After that, the zymograms were incubated for 18 h at 37 °C in the incubation buffer (5 mM $CaCl_2$, 50 mM Tris–HCl pH 7.5, 1 mM $ZnCl_2$). After incubation, the gels were fixed with methanol:acetic acid:water (4.5:1:4.5, v/v) for 15 min at room temperature with moderate agitation. The gels were then stained with 0.1% Coomassie Brilliant Blue G-250 and were destained with methanol:acetic acid:water (4.5:1:4.5, v/v). The areas of enzymatic activity appeared as clear bands over the dark background.

Measurement of IL-1β production

Renca cells were trypsinized, counted, and 1×10^6 cells were transferred into 6-well flasks with 4 mL of RPMI without serum. After 24 h, the conditioned media was transferred into 1.5-mL tubes, centrifuged ($300 \times g$) to remove cellular debris, and the resulting supernatants were filtered using 0.22 µm disposable TPP syringe filters (Techno Plastic Products, Trasadingen, Switzerland) and were stored at − 20 °C until they were assayed for IL-1β.

The concentrations of IL-1β in the supernatants of the Renca cell cultures were determined using an ELISA kit according to the manufacturer's instructions (Invitrogen, Carlsbad, CA).

Statistical analysis and protein–protein interaction map

Simple comparisons of the means were performed by Student's t test. The results of the present study are presented as the mean $\pm$ SDs. Multiple mean comparisons were performed using one–way analysis of variance (ANOVA) followed by Bonferroni's test using GraphPad Prism 6.0 (GraphPad Software, Inc., La Jolla, CA, USA). $P < 0.05$ indicated a statistically significant difference. All experiments were performed in triplicates. A protein–protein interaction map was generated using the STRING v11.0 website by inputting the following proteins: NFκB1, MMp-9 and IL-1. The results were set to display up to ten interactions [20].

Results

Expression of p105 and p50 proteins decreased significantly in Renca-shRNA-NF-κB1 cells

First, the NF-κB1 gene knockdown effect on the protein level was evaluated by western blotting. The results revealed that the expression of p105 and p50 in Renca-shRNA-NF-κB1 cells was reduced by $84 \pm 0.01\%$ ($P < 0.01$) and $77 \pm 0.08\%$ ($P < 0.001$), respectively (Fig. 1a, b). In all experiments, Renca non-target shRNA transduced cells (Renca–mock) were used as controls.

Silencing of NF-κB1 inhibited the clonogenic capacity of RCC cells

To determine whether NF-κB1 is required for the clonogenic growth of Renca cell lines, the cells were plated and maintained in culture for 10 days with or without knockdown. NF-κB1 knockdown led to the inhibition of colony formation. The colony numbers of shRNA-NF-κB1 cells (49.0 ± 1.0/plate) were significantly lower than those of the Renca–mock control group (69.33 ± 4.0/plate) ($P < 0.01$ vs Renca–mock) (Fig. 2a and b).

Silencing of NF-κB1 inhibits the migration and invasion of Renca cells

To establish whether the decreased NF-κB1 levels would impact the migration of Renca cells, a wound healing assay and a transwell migration assay were performed. Wound healing assay results (Fig. 3a) demonstrated that NF-κB1 knockdown produced a 10% inhibition of Renca-shRNA-NF-κB1 cell migration ($P < 0.01$ vs. Renca mock). (Figure 3a1). This finding was Corroborated by those obtained by transwell migration assay where the number of Renca-shRNA-NF-κB1 cells that had migrated decreased by 0.5-fold compared with the number of Renca–mock cells ($P < 0.001$ vs. Renca mock) (Fig. 3b, b1). The invasion ability was assessed using a transwell assay (Fig. 3c). The number of Renca-shRNA-NF-κB1 cells penetrating the membrane decreased by 0.6-fold compared with the number of Renca–mock cells ($P < 0.001$ vs. Renca mock) (Fig. 3c1).
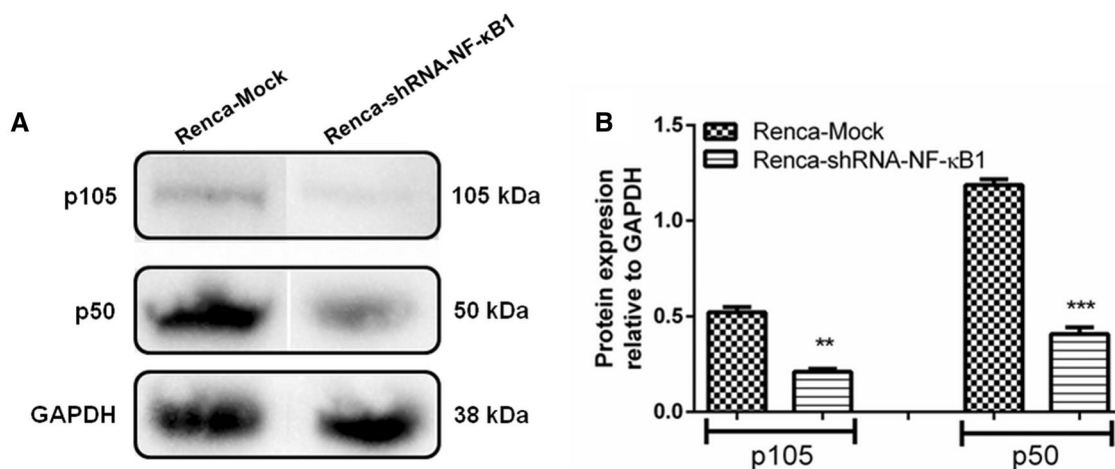

Fig. 1 Stable knockdown of NF-κB1 in Renca cells. **a** Western blotting analysis. The optical density values of the corresponding bands were quantified by ImageJ software, and GAPDH was used as an internal control. **b** The results show a reduction of p105 protein (**$P < 0.01$ vs Renca–mock) and p50 (***$P < 0.001$ vs Renca–mock)
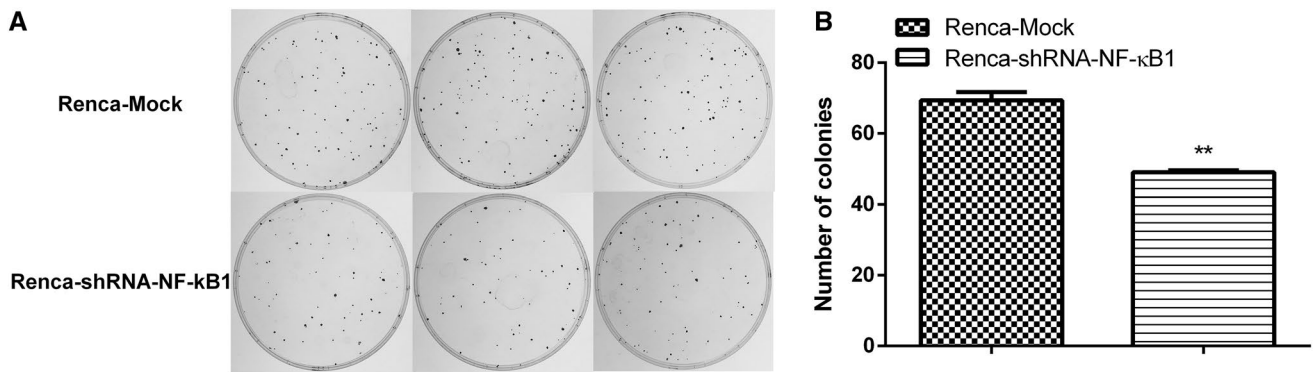
Fig. 2 shRNA-mediated knockdown of NF-κB1 inhibited the clonogenic capacity of Renca cells. **a** Representative images of stained colonies. **b** Quantitative analysis revealed a significant difference between Renca–mock and the Renca-shRNA-NF-κB1 ($P < 0.05$). (**$P < 0.01$ vs Renca–mock) Values are the mean $\pm$ SD; $n = 3$

Knockdown of NF-κB1 inhibited IL-1β mRNA expression and protein production by Renca cells

The effect on the production of *IL-1β*, a known target gene of *NF-κB*, by Renca-shRNA-NF-κB1 cells was evaluated. The *IL-1b* mRNA production was assessed by RT-qPCR, demonstrating lower expression levels in the Renca-shRNA-NF-κB1 cells, with an mRNA-level reduction of $98.3 \pm 0.11\%$ ($P < 0.001$) compared to that of the Renca–mock cells (Fig. 4a). Protein expression was verified by ELISA assays using culture media and western blotting of cell protein extracts. Corroborating the RT-qPCR data, the *IL-1β* expression in the Renca-shRNA-NF-κB1 culture media was 0.39 ± 0.01 pg/mL whereas mock cells showed 9.58 ± 0.27 pg/mL ($P < 0.001$) (Fig. 4b). As expected, the western blotting analysis revealed a reduction of *IL-1β* by $92.13 \pm 0.55\%$ compared to that in the Renca–mock cells ($P < 0.001$) (Figs. 4c, d).

Knockdown of NF-κB1 downregulated MMP-9 expression and activity by Renca cells

MMP-9 expression was assessed by *RT-qPCR* and western blotting analyses. NF-κB1 mRNA expression decreased by $89.00 \pm 0.05\%$ compared to that in the Renca–mock cells ($P < 0.001$) (Fig. 5a). This was further corroborated by western blotting, revealing a decrease in active MMP-9 (86 kDa) by approximately $49.4 \pm 0.57\%$ ($P < 0.01$) (Fig. 5b, c). Furthermore, the gelatinolytic activity of MMP-9 was also significantly decreased in the Renca-shRNA-NF-κB1 cells (Fig. 5d). Corroborating all these findings, a protein interaction map was generated using the STRING website and provided evidence of the interaction between NF-κB1, MMP-9 and IL-1.

Discussion

NF-κB is a very important transcription factor, is ubiquitously expressed in many different cell types, and orchestrates several cellular and molecular mechanisms, mainly those involved in the immune response because most toll-like receptors and several cytokines signalling pathways converge for NF-κB translocation into the nucleus [8]. Of further interest, clinical evidence has suggested that nuclear NF-κB also plays a crucial role in tumour cell functions, such as proliferation, migration, and apoptosis [21]. An altered expression of NF-κB in solid tumours has been correlated with poor prognosis and resistance to antineoplastic treatments [11, 22].

In this report, we demonstrate that the colony formation ability, as well as the migration and invasion capacity of Renca-shRNA-NF-κB1 cells, were significantly impaired; this was likely due to a reduction in MMP-9 activity as well as other NF-κB target genes. The results from the western blots revealed that p105/p50 protein expression was efficiently downregulated in these cells. The strategy of using an shRNA to successfully reduce the expression of a target gene has been widely used [23, 24].

Renca-shRNA-NF-κB1 cells presented with decreased colony formation, indicating that NF-κB1 mediates the proliferative potential of Renca colony-forming cells. However, whether this is a direct effect of NF-κB inhibition on cell cycle-related genes has not been addressed. In fact, NF-κB1 may directly target several genes that modulate cell survival and proliferation, such as Cyclins and MAP kinases (Fig. 5e). Thus, it is possible that NF-κB1 inhibition in Renca-shRNA-NF-κB1 cells could lead to the reduced expression of such genes, impairing cell viability and expansion.
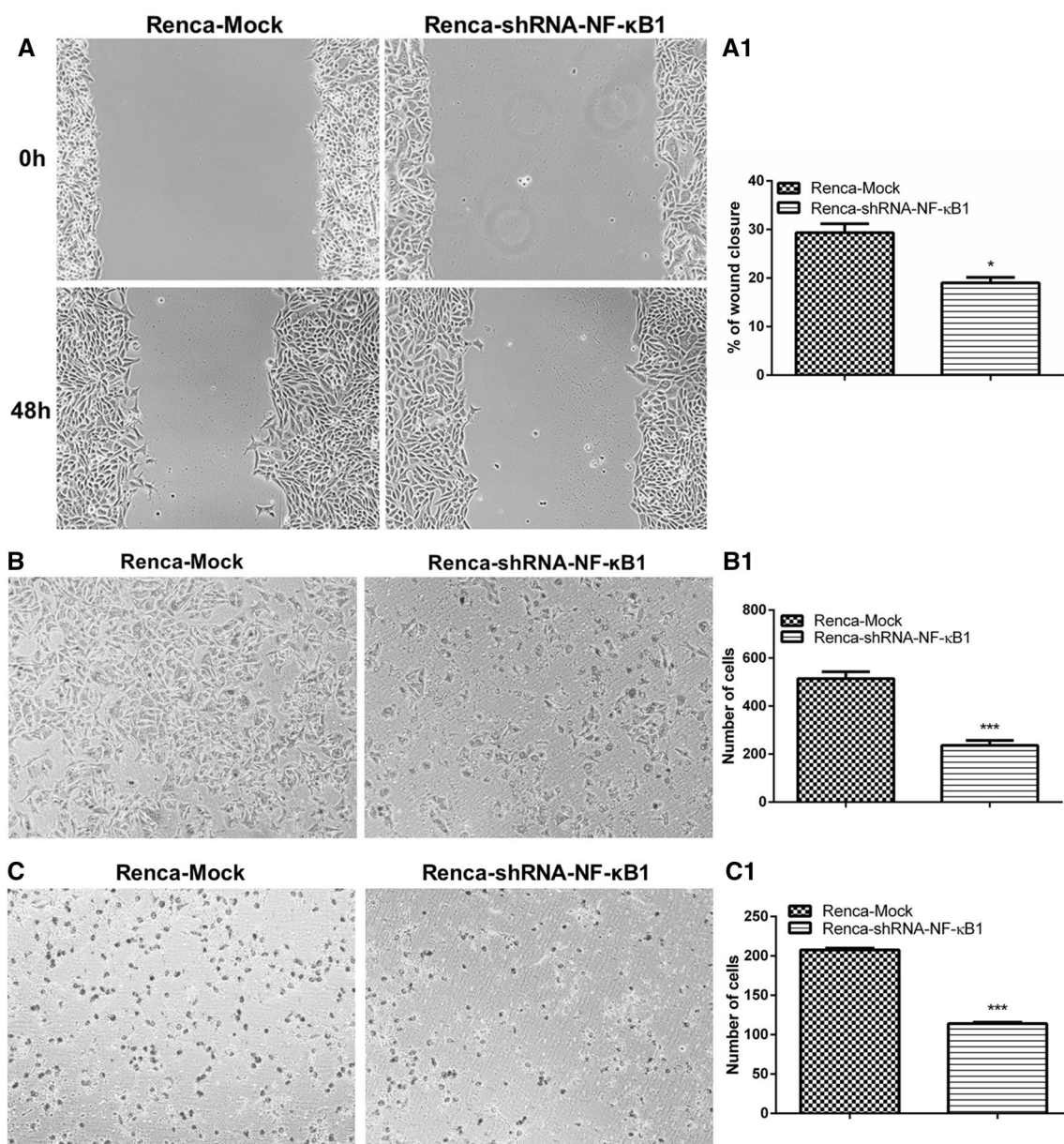
Fig. 3 NF-κB1-knockdown inhibits Renca cell migration and invasion. **a** The migration of Renca cells was assessed by a wound-healing assay. Representative images of wound closure were taken at 0 h and 48 h after wounding under ×100 magnification. **a1** Cell migration was quantified and represented in a Bar graph (*P < 0.05 vs Renca–mock). **b** Assessment of cell migration by transwell assay. Representative image of migration by transwell assay. **B1** migration was quantified and represented in a Bar graph (P < 0.001 vs. Renca–mock) (**b1**). **c** Representative images of the invasion assay, **c1** Cell invasion was quantified and represented in a Bar graph (***P < 0.001 vs Renca–mock). Values are the mean ± SD; n = 3

On the other hand, NF-κB may also have an indirect impact on the aforementioned phenomenon. It has been shown that during cancer, several tumoural growth factors are secreted, either by the tumour cells themselves or by nearby host cells [25, 26]. Here, we show that Renca-shRNA-NF-κB1 cells exhibited a decreased IL-1 response compared to that of Renca-shRNA-cells. IL-1 is a very important cytokine for the innate immune response, not only against pathogens but also against tumour cells. IL-1 secretion follows a complex and orchestrated molecular mechanism called pyroptosis, which is dependent on inflammasome assembly and the cleavage of pro-IL-1beta in the cytoplasm [26, 27]. Interestingly, it has been shown that IL-1 may also act as a tumour growth factor, boosting tumour cell growth and survival [10]. Thus, it is plausible that Renca-shRNA-NF-κB1 cells have not only a reduced IL-1
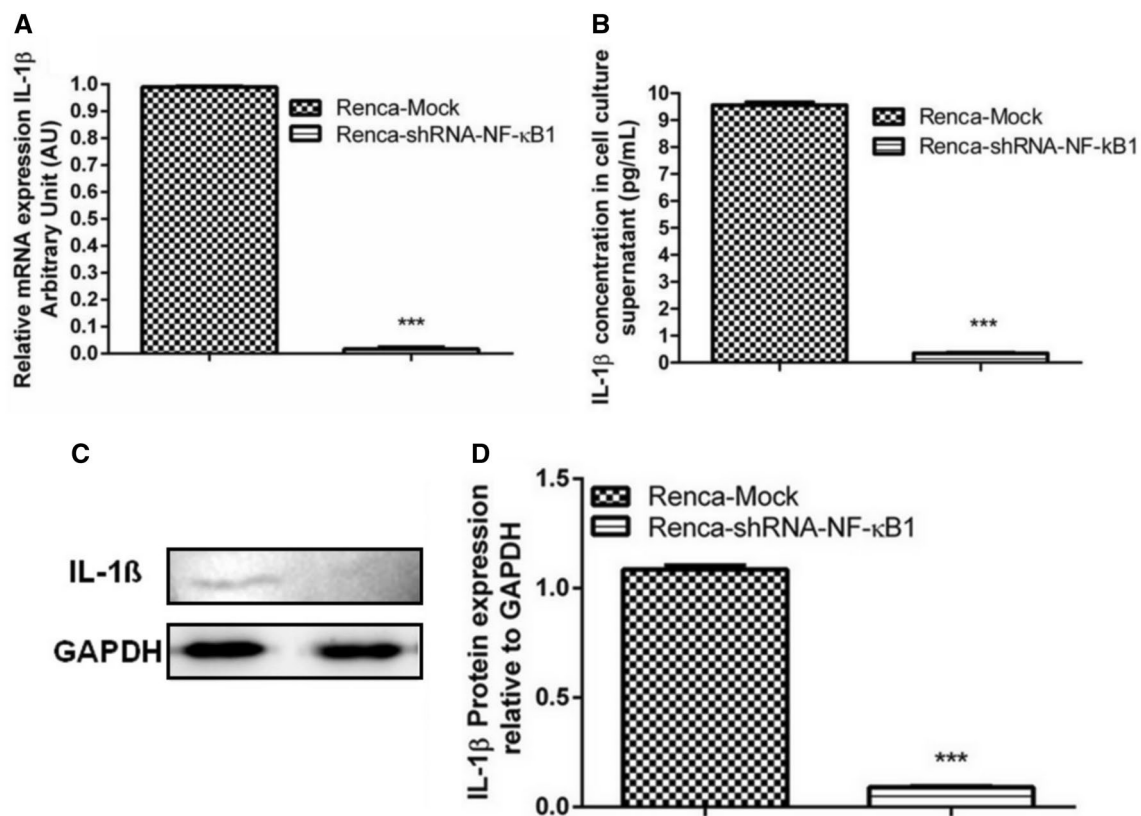
Fig. 4 NF-κB1-knockdown inhibited IL-1β expression. **a** RT-PCR analysis. **b** Determination of IL-1β concentration in the supernatants of Renca cell culture. (***P < 0.001 vs Renca–Mock). **c** Western blotting analysis. The optical density values of the corresponding bands were quantified by ImageJ software, and GAPDH was used as an internal control. **d** The results show a reduction of IL-1β protein (***P < 0.001 vs Renca–mock). Values are the means ± SD; n = 3

secretion level, but also an impaired signalling pathway, as IL-1 activates the IL-1R signalling pathway that also results in NF-κB1 translocation. However, these implications must be addressed in vivo because, as already mentioned, IL-1 has an important anti-tumoural function, mainly by recruiting inflammatory cells.

In addition, our data show that the low levels of NF-κB p50 caused a significant decrease in the cell migration and invasion of Renca cells. This is due to a decrease in the expression of MMP-9, an important metastasis promoting factor. The promoter of MMP-9 has responsive elements for several different transcriptional factors, including AP-1, SP-1, Ets and NF-κB [28]; this is evidence for a direct correlation between them. Accumulated data have correlated the enhanced expression of MMP-9 with the activation of NF-κB and metastasis [18, 29]. MMP-9 is an endopeptidase with three fibronectin Type II domains that confer higher affinity for its collagen substrate [30]. This activity helps degrade the extracellular matrix, allowing metastatic cells to detach from the primary tumour and to gain access to the circulation, leading to metastasis. Moreover, MMP-9 may also act on endothelial cells, facilitating the carcinogenesis

of skin cells and the spread throughout the body [31]. Thus, consistent with these findings, we have shown that NF-κB1 abrogation led to reduced MMP-9 secretion, impairing Renca cells to migrate in Transwell assays. Although it has already been shown in the literature that NF-κB acts on MMP-9 transcription, it is worth mentioning that we also observed a significant reduction of MMP-9 activity after NF-κB1 knockdown, probably due to the reduced level of this molecule in the supernatant.

As mentioned, IL-1 also signals through NF-κB1. Thus, IL-1 signalling pathway impairment by shRNA-NF-κB1 in Renca cells may also account for the overall suppression of MMP-9 secretion. In addition, a published meta-analysis on ccRCC gene expression was performed by Suraj Peri and collaborators and identified that the elevated expression of MMP-9 was significantly associated with a higher relative risk, poorer prognosis, and reduced survival for RCC patients [32].

In summary, our data, presented here, show the role of NF-κB1 in orchestrating the proliferation and metastatic potential of RCC cells in vitro. As mentioned, RCC accounts for 90–95% of kidney cancer cases, of which, 25–30% of
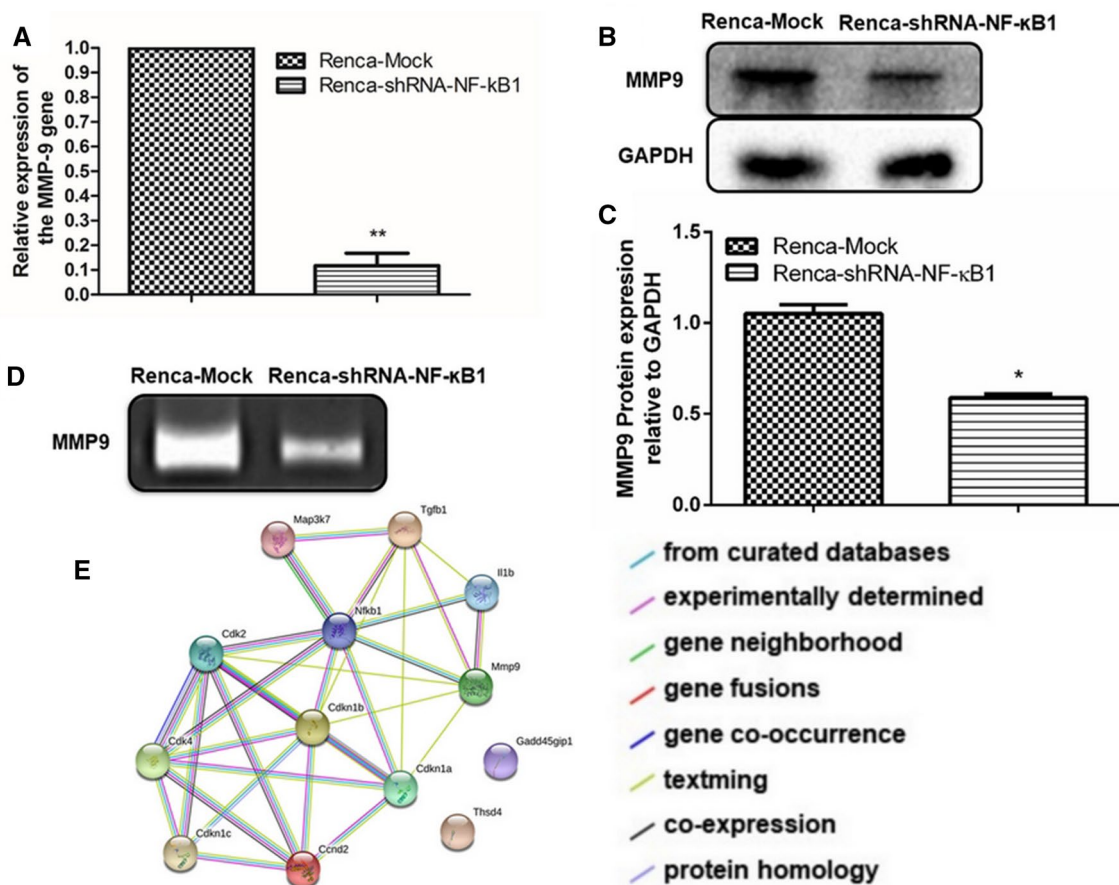
Fig. 5 NF-κB1-knockdown downregulated MMP-9 expression and activity. **a** RT-PCR analysis. **b** Western blot analysis. **c** The optical density values of the corresponding bands were quantified using ImageJ software, with ß-actin serving as an internal control. The results show a reduction in MMP-9 at the protein level (*P < 0.01 vs Renca–mock). **d** MMP-9 Gelatinase activity in 48 h conditioned medium from Renca–mock and Renca-shRNA-NF-κB1 cells. **e** Protein Interaction Maps elaborated using STRING website shows direct interaction between NFκ-B1, MMP-9 and IL-1

patients develop metastasis after surgery. This evidence supports the clinical importance of RCC as well as the importance of understanding its biology. The relevance of our findings in vivo was not addressed, but it is one of our further goals. Both IL-1 and MMP-9 seem to have a dual role in vivo, as both may boost the immune response [26], facilitating the recruitment of inflammatory cells and promoting tumoural growth and metastasis. This is clinically corroborated, as bladder tumours may be treated by the intravesical inoculation of BCG (Bacille Calmette-Guérin), a robust immune stimulus of pro-inflammatory cytokines, including IL-1.

Conclusion

The knockdown of NF-κB1 renal tumour cells significantly reduced the potential for colony formation, expansion and cellular migration in vitro. These findings correlate with the downregulation of IL-1 and MMP-9 secretion, as well as with MMP-9 activity, indicating a possible molecular mechanism for NF-κB1 in the development and progression of RCC. Finally, this study suggests that NF-κB1 could be a molecular target for RCC therapy.

Compliance with ethical standards

Conflict of interest On behalf of all authors, the corresponding author states that there is no conflict of interest.

References

1. Gao Y, Li H, Ma X, Fan Y, Ni D, Zhang Y, Huang Q, Liu K, Li X, Wang L, Gu L, Yao Y, Ai Q, Du Q, Song E, Zhang X (2017)

KLF6 Suppresses metastasis of clear cell renal cell carcinoma via transcriptional repression of E2F1. Cancer Res 77:330–342

2. Foguer K, Braga MS, Peron JPS, Bortoluci KR, Bellini MH (2016) Endostatin gene therapy inhibits intratumoral macrophage M2 polarization. Biomed Pharmacother 79:102–111

3. Kim W, Zachary G, Daaka Y (2012) Rap1GAP regulates renal cell carcinoma invasion. Cancer Lett 320(1):65–71

4. Zarrabi K, Fang C, Wu S (2017) New treatment options for metastatic renal cell carcinoma with prior anti-angiogenesis therapy. J Hematol Oncol 10(1):38

5. Shenoy N, Pagliaro L (2016) Sequential pathogenesis of metastatic VHL mutant clear cell renal cell carcinoma: putting it together with a translational perspective. Ann Oncol 27:1685–1695

6. An J, Rettig MB (2005) Mechanism of von Hippel-Lindau protein-mediated suppression of nuclear factor kappa B activity. Mol Cell Biol 25(17):7546–7556

7. Karin M (2009) NF-κB as a critical link between inflammation and cancer. Cold Spring Harb Perspect Biol 1(5):a000141

8. Zhang Q, Lenardo MJ, Baltimore D (2017) 30 Years of NF-κB: a blossoming of relevance to human pathobiology. Cell 168(1–2):37–57

9. Voronov E, Carmi Y, Apte RN (2014) The role IL-1 in tumor-mediated angiogenesis. Front Physiol 5:114

10. Braga MS, Foguer K, Chaves KCB, Lima LS, Scavone C, Bellini MH (2014) Involvement of the NF-κB/p50/Bcl-3 complex in response to antiangiogenic therapy in a mouse model of metastatic renal cell carcinoma. Biomed Pharmacother 68:873–879

11. Lewis AM, Varghese S, Xu H, Alexander HR (2006) Interleukin-1 and cancer progression: the emerging role of interleukin-1 receptor antagonist as a novel therapeutic agent in cancer treatment. J Transl Med 4:48

12. Oya M, Takayanagi A, Horiguchi A, Mizuno R, Ohtsubo M, Marumo K, Shimizu N, Murai M (2003) Increased nuclear factor-kappa B activation is related to the tumor development of renal cell carcinoma. Carcinogenesis 24:377–384

13. Meteoglu I, Erdogdu IH, MeydanN Erkus M, Barutca S (2008) NF-KappaB expression correlates with apoptosis and angiogenesis in clear cell renal cell carcinoma tissues. J Exp Clin Cancer Res 27:53

14. Cai H, Sun L, Cui L, Cao Q, Qin C, Zhang G, Mao X, Wang M, Zhang Z, Shao P, Yin C (2013) A functional insertion/deletion polymorphism (-94 ins/del ATTG) in the promoter region of the NFKB1 gene is related to the risk of renal cell carcinoma. Urol Int 91(2):206–212

15. Gupta SC, Kim JH, Prasad S, Aggarwal BB (2010) Regulation of survival, proliferation, invasion, angiogenesis, and metastasis of tumor cells through modulation of inflammatory pathways by nutraceuticals. Cancer Metastasis Rev 29(3):405–434

16. Kessenbrock K, Plaks V, Werb Z (2010) Matrix metalloproteinases: regulators of the tumor microenvironment. Cell 141(1):52–67

17. Roomi MV, Ivanov V, Kalinovsky T, Niedzwiecki A, Rath M (2006) Modulation of human renal cell carcinoma 786-0 MMP-2 and MMP-9 activity by inhibitors and inducers in vitro. Med Oncol 23(2):245–250

18. Lin YW, Lee LM, Lee WJ, Chu CY, Tan P, Yang YC, Chen WY, Yang SF, Hsiao M, Chien MH (2016) Melatonin inhibits MMP-9 transactivation and renal cell carcinoma metastasis by suppressing Akt-MAPKs pathway and NF-κB DNA-binding activity. J Pineal Res 60(3):277–290

19. Ikegami A, Teixeira LFS, Braga MS, Dias MHS, Lopes EC, Bellini MH (2018) Knockdown of NF-κB1 by shRNA inhibits the growth of renal cell carcinoma in vitro and in vivo. Oncol Res 26(5):743–751

20. Szklarczyk D, Morris JH, Cook H, Kuhn M, Wyder S, Simonovic M, Santos A, Doncheva NT, Roth A, Bork P et al (2017) The STRING database in 2017: quality-controlled protein-protein association networks, made broadly accessible. Nucleic Acids Res 45(D1):D362–D368

21. Bosman MC, Schuringa JJ, Vellenga E (2016) Constitutive NF-κB activation in AML : causes and treatment strategies. Crit Rev Oncol Hematol 98:35–44

22. Scartozzi M, Bearzi I, Pierantoni C, Mandolesi A, Loupakis F, Zaniboni A, Catalano V, Quadri A, Zorzi F, Berardi R, Biscotti T, Labianca R, Falcone A, Cascinu S (2007) Nuclear factor-kB tumor expression predicts response and survival in irinotecan-refractory metastatic colorectal cancer treated with cetuximab-irinotecan therapy. J Clin Oncol 25(25):3930–3935

23. Habib R, Akhtar J, Taqi M, Yu C, Zhang C (2015) Lentiviral vector-mediated survivin shRNA delivery in gastric cancer cell lines significantly inhibits cell proliferation and tumor growth. Oncol Rep 34(2):859–867

24. Zhong MA, Zhang H, Qi XY, Lu AG, You TG, Gao W, Guo XL, Zhou ZQ, Yang Y, Wang CJ (2011) ShRNA-mediated gene silencing of heat shock protein 70 inhibits human colon cancer growth. Mol Med Rep 4(5):805–810

25. Qian BZ, Pollard JW (2010) Macrophage diversity enhances tumor progression and metastasis. Cell 141:39–51

26. Curiel TJ, Coukos G, Zou L, Alvarez X, Cheng P, Mottram P, Evdemon-Hogan M, Conejo-Garcia JR, Zhang L, Burow M, Zhu Y, Wei S, Kryczek I, Daniel B, Gordon A, Myers L, Lackner A, Disis ML, Knutson KL, Chen L, Zou W (2004) Specific recruitment of regulatory T cells in ovarian carcinoma fosters immune privilege and predicts reduced survival. Nat Med 10(9):942–949

27. Latz E (2010) The inflammasomes: mechanisms of activation and function. Curr Opin Immunol 22:28–33

28. Chen CY, Hsiao HL, Yang CM (2012) PI3-K/Akt/JNK/NF-κB is essential for MMP-9 expression and outgrowth in human limbal epithelial cells on intact amniotic membrane. Stem Cell Res 9(1):9–23

29. Tang D, Tao D, Fang Y, Deng C, Xu Q, Zhou J (2017) TNF-alpha promotes invasion and metastasis via NF-Kappa B pathway in oral squamous cell carcinoma. Med Sci Monit Basic Res 23:141–149

30. Kridel SJ, Chen E, Kotra LP, Howard EW, Mobashery S, Smith JW (2001) Substrate hydrolysis by matrix metalloproteinase-9. J Biol Chem 276(23):20572–20578

31. Coussens LM, Tinkle CL, Hanahan D, Werb Z (2000) MMP-9 supplied by bone marrow derived cells contributes to skin carcinogenesis. Cell 103(3):481–490

32. Peri S, Devarajan K, Yang DH, Knudson AG, Balachandran S (2013) Meta-analysis identifies NF-κB as a therapeutic target in renal cancer. PLoS ONE 8(10):e76746